Energetics of vacancy and substitutional impurities in aluminum bulk and clusters

D. E. Turner*
Ames Laboratory, U.S. Department of Energy, Department of Physics and Astronomy, Iowa State University, Ames, Iowa 50011

Z. Z. Zhu
Xiamen University, Department of Physics, Fujian 361005, China

C. T. Chan
Department of Physics, Hong Kong University of Science and Technology, Clear Water Bay, Hong Kong

K. M. Ho
Ames Laboratory, U.S. Department of Energy, Department of Physics and Astronomy, Iowa State University, Ames, Iowa 50011
(Received 1 November 1996)

We present a careful study of the energetics of vacancy and substitutional impurities in aluminum in both the bulk and small cluster environments. The calculations are done within the framework of the local-density-functional formalism and are based on the pseudopotential method with plane-wave expansion and periodic boundary conditions. Both the ionic and electronic degrees of freedom are fully relaxed. The electronic structure problem is treated with a preconditioned conjugate-gradient method that applies equally well to insulators and metals, and is suitable for parallel computing. We have considered up to 216 atoms in the supercell, and we show that reliable results can be obtained with 108-atom cells with proper **k**-point sampling. Vacancy-formation energy, heats of solution of the impurities and the relaxations near the defects are in good agreement with available experimental data. The energetics of substitution in small clusters was found to be rather different from bulk. [S0163-1829(97)07320-7]

I. INTRODUCTION

Point defects and impurities are the simplest defects in a solid. Nevertheless, a great number of physical and mechanical properties are sensitive to their presence. A detailed knowledge of point defects is thus essential for understanding the atomistic as well as the macroscopic behavior of materials. In the past, it has been customary to study defects and impurities with empirical potential models,[1,2] but in recent years it has been increasingly popular to apply *ab initio* calculations to study these systems, especially for defect formation energies in simple metals.[3–8] Although first-principles calculations are inevitably slower and far fewer atoms can be handled than by empirical methods, there are still good reasons to use *ab initio* techniques. One major reason is that whereas reliable empirical model interactions may be available for one particular element in some particular physical or chemical environment, it is difficult to find a model potential that applies to all occasions. The situation becomes even more intractable if the system contains more than one component. For example, it would be rather difficult to use an empirical or semiempirical technique to study the energetics of substitutional defects of Si in Al, even though Al on its own may be well described by embedded-atom-type interactions in the bulk, and Si in the bulk diamond structure can be represented well using a simple tight-binding model. If we take on the more challenging task of studying the Si interaction with Al in very different environments such as in bulk and small clusters, empirical potentials that were designed to work in the bulk will probably fail in the cluster environment. The first-principles local-density-functional method (LDA), on the other hand, is sufficiently accurate for multicomponent systems in drastically different chemical environments. Although LDA studies are currently limited to a few hundred atoms, a lot of important results about the energetics of defect formation can already be obtained. In addition, the first-principles results can generate a large amount of information about the interatomic interaction on a microscopic scale that can used to fit, or at least put constraints on, simple interatomic potentials. It is difficult, if not impossible, to extract such information from experiments.

The last few years have witnessed great advances in the ability to calculate the structure and energy of solids by the use of density-functional theory within the LDA framework.[9] As far as the computation technique is concerned, an important milestone is the development of the Car-Parrinello method.[10] This method treats the electronic degrees of freedom as classical entities, and puts the electronic and ionic degrees of freedom on the same footing. By proper choice of the fictitious mass of the electronic degrees of freedom, first-principles molecular dynamics can be performed. If we freeze the ionic degrees of freedom, the electrons can find their ground state through an annealing process if the temperature is reduced slowly, or through a steepest-decent procedure if the problem is treated as molecular statics. This is not just a technical innovation, but actually opens up new ways of thinking about total energy calculations, and has stimulated the development of alternative ways of handling the electronic structure problems. Another important development is the preconditioned conjugate-gradient method,[11–13] which treats the electronic degrees of freedom

as a problem of constrained minimization of the total energy of the Kohn-Sham functional. Both methods have significantly improved the capability and thus the applicability of local-density-functional methods to problems of practical interest. These developments are further augmented by the rapid progress in parallel computing hardware and techniques.[13–16] Using these methods, one can now perform calculations for systems containing hundreds of atoms for semiconductors.[14,15]

In the conjugate-gradient method, one minimizes a function of many variables by first computing the gradient of the object function. The gradient is then used to construct a vector of change that is added to the original trial vector in such an amount as to minimize the function. This process is repeated with each new vector being forced to be conjugate to the previous change vectors. The conjugate-gradient technique, with pre-conditioning, is applied by Teter, Payne, and Allan[11] to minimize the total energy of the local density functional in a band-by-band manner. This approach works well for insulators and semiconductors, but metallic systems are not as easy to deal with. The occupancies for each band are known for insulators and semiconductors, while they must be determined for metallic systems. For semiconductors, we only need to find the subspace that is spanned by the eigenvectors (i.e., linear combination of eigenvectors are as good as the eigenvectors when we need to know the charge density and the sum of eigenvalues of the occupied states), which offers more flexibility for an optimization scheme. But for metals, knowing the sum of the eigenvalues (the trace of the Hamiltonian within the subspace spanned by the occupied states) is not enough, we need to know the individual eigenstates and eigenvalues before we can determine the occupancy. In addition, **k**-point sampling is more demanding in metallic systems, so that whatever method we use has to have the capability of treating many **k** points, and the sampling must be done adequately and be carefully monitored. Chetty *et al.*[8] have shown that even for systems containing more than 100 atoms, the calculated vacancy formation energy can have a wrong sign if only the Γ point is used.

In this paper, we will show that metals can be treated on an equal footing with semiconductors with some modification of the original preconditioned conjugate-gradient scheme. The calculations are centered around aluminum, which is taken to be the prototypical simple metal and because of the importance of aluminum and its alloys in industrial applications. Aluminum is the world's second most commonly used metal and there is a wide and varied family of aluminum alloys now used for a multitude of purposes throughout the aeronautics, space exploration, and electronics industries.

This paper is arranged as follows. Section II describes the methods employed for achieving the ground state of the electronic and ionic degrees of freedom. In Sec. III, the calculated results for vacancy formation energies and the energetics of impurities of Si, Mg, and Li in Al will be presented. We also present results of substituting Al by the same elements Si, Mg, and Li, but in a small cluster environment instead of in bulk aluminum. A summary is given in Sec. V.

II. CALCULATION METHOD

Our calculations are performed within the local-density-functional formalism[9] using the Hedin-Lundqvist form for the exchange-correlation potential[17] and a plane-wave basis set.

Calculating the vacancy formation energy involves both the relaxation of electrons to the self-consistent ground state and the relaxation of the ions to their equilibrium positions. Our method for relaxing the electronic degrees of freedom is a variation of the preconditioned conjugate-gradient scheme of Teter, Payne, and Allen.[11] The original conjugate-gradient method of Teter, Payne, and Allen is an iterative band-by-band constrained minimization of the LDA total energy functional. We instead iteratively minimize the sum of the eigenvalues for a fixed number of bands. The trial vectors are varied, subject to orthonormal constraints, so as to minimize the sum of the eigenvalues for the lowest N bands for the fixed Hamiltonian with a fixed input potential. For metallic systems, the number N has to be large enough to cover all the bands so that the fractional occupation number is not negligibly small. The set of vectors that optimize the sum of eigenvalues for a fixed number of N bands spans the same subspace as the N eigenvectors, but a subspace diagonalization is needed to rotate the subspace to that of the eigenvectors and find the eigenvalues of the individual levels. In our calculations of up to 108 atoms, the subspace diagonalization takes less than 5% of the computation time.[18] This process is a conjugate-gradient iterative diagonalization procedure. When the eigenvalues are known, the Fermi level can be determined (by assuming a particular value of the Gaussian broadening) and the occupation of the levels is then found. The charge density can then be determined since we know the eigenvectors and the occupation number. The whole process is then repeated until we reach self-consistency between input and output screening potentials. As for the relaxation of the electronic degrees of freedom, we are operating with a fixed Hamiltonian and the minimization procedure uses a simpler conjugate-gradient scheme than the original conjugate-gradient scheme proposed by Teter and co-workers[11,13] where the Hamiltonian changes as each band gets updated. In our approach there is no need to compute the change in the charge and potential as the optimization procedure goes through band by band and **k** point by **k** point. In addition, the line minimization for the trial vector [corresponding to Eq. (5.23) of Payne *et al.*[13]] is more straightforward for a fixed Hamiltonian. The advantage of this approach is that metals and semiconductors are put on an equal footing. The price we have to pay is that we have to achieve self-consistency between the charge and potential, but we have had no difficulty in reaching self-consistency in the potential using a Broyden scheme[19] for systems we have treated here, including vacancies and substitutional defects in Al with fairly large unit cells. We note that attaining self-consistency can be much more demanding for certain transition metals with high density of states near the Fermi level, and for systems with even larger unit cells. In those systems, it is inevitable that more computational effort has to be spent in achieving self-consistency. This should not be regarded as a deficiency of the present method, but rather that some systems are intrinsically more difficult than the others. If we directly minimize the total energy, we apparently can by pass the self-consistency problem. However, there is no guarantee, especially for metallic systems, that the passage to the

TABLE I. The unrelaxed vacancy-formation energy as a function of system size for a small set of 182 **k** points and a large set of 1300 **k** points (0.20-eV band energy smearing).

Atoms per supercell	Structure	Equivalent **k** points	Small set energy (eV)	Equivalent **k** points	Large set energy (eV)
1	fcc	182		1300	
4	sc	56	0.736	364	0.743
8	fcc	28	0.755	182	0.766
16	bcc	20	0.750	112	0.774
27	fcc	10	0.689	60	0.758
32	sc	10	0.678	56	0.756
64	fcc	6	0.644	28	0.732
108	sc	4	0.661	20	0.735

final ground state is more efficient than the scheme we employed here.

In the relaxation of the ionic configurations, we employed the force matrix method in which atomic positions are updated by $\delta\mathbf{X}=K^{-1}\cdot\mathbf{F}$, where $\mathbf{F}$ are the Hellmann-Feynman forces and K is the force matrix. For vacancy calculations, which involve radial displacements, there are only a few degrees of freedom and the elements of the force matrix are found initially using finite differences from small displacements of the atoms. It is further refined as the atoms are displaced using the Broyden method.[19] We also employed a conjugate-gradient scheme in relaxing the atomic positions. Although this conjugate-gradient relaxation takes more steps to relax the atoms, it is eventually preferred since it allows the whole relaxation process to be fully automated.

We also note that it is not necessary to fully optimize the electron trial wave functions before we update the electron screening potential. Initially, when we have reasonably good electron screening potentials (constructed from a superposition of atomic charges) but poor wave functions, we perform approximately six conjugate-gradient steps before we update the potential. When the wave functions get better, only 2–3 conjugate-gradient steps are executed before updating the potential. It is also not necessary to fully relax the electronic degrees of freedom or wait until the potential becomes fully consistent before proceeding to move the atoms. The error in the forces due to the error in self-consistency can be corrected and the change in the potential due to the change of the atomic positions can be predicted rather effectively by a recently proposed scheme.[20]

Most of the results reported here employ a simple-cubic supercell with $L=3\mathbf{a}$, where L is the supercell dimension and $\mathbf{a}$ is the lattice constant of fcc bulk aluminum. There are 108 atomic sites per supercell. Tests were done using up to 216 atom cells to test for size effects. The Kleinman-Bylander-type pseudopotentials[21] were generated according to the coefficients presented by Stumpf and co-workers.[22] The d-wave component of the pseudopotential is set as the local potential and the s and p components were treated as nonlocal potentials. The Bloch wave functions are represented by a plane-wave basis using a 12.5-Ry cutoff for the plane-wave kinetic energy. The equilibrium lattice constant and cohesive energy are 3.97 Å and 3.96 eV, respectively, for fcc Al, which compare well with experimental values of 4.05 Å and 3.39 eV.[23] The four special **k** points in the 1/48 irreducible Brillouin zone provide a reasonable precision at a moderate cost in the present supercell with 108 atomic sites. This choice of **k** points and system size are discussed in full detail in a later section.

The present method relies on the efficiency of fast Fourier transformations and is suitable for implementation on massively parallel computers. Most of the computations presented here were performed on a machine with a parallel architecture (nCube 2S). The parallelization strategy basically involves spreading real space and reciprocal space across the nodes.[24] This divides both the CPU load and the memory requirements equally among the nodes. Communication between nodes is necessary during the transformation between real and reciprocal space. This is handled using a highly tuned three-dimensional fast Fourier transform (3D FFT) algorithm that takes advantage of the fact that the reciprocal-space representation is localized to a sphere. The efficiency of the 3D FFT algorithm allows the problem to be spread over twice as many nodes as the length of the side of the mesh. Calculations involving multiple **k** points can also take advantage of this higher level of parallelism by running each **k** point concurrently on a subset of the available nodes. For example, a typical 4-**k**-point calculation of aluminum on a $64\times64\times64$ mesh can run with 87% efficiency on 256 nodes by running each **k** point on a 64-node subset where the distributed 3D FFT operates with high efficiency.

III. RESULTS AND DISCUSSIONS

A. k-point sampling, supercell size, and pseudopotentials

Since we are handling metallic systems, which are usually more demanding on the system size and **k**-point sampling than semiconductors or insulators, we first studied the effects of the system size, the number of **k** points used, and the Gaussian band smearing[25] on the calculated vacancy formation energy. Chetty *et al.*[8] have emphasized that a large **k**-point set must be used to accurately calculate the defect energies in Al, even when large supercells are used to ensure that the defects are very far apart. This is in opposition to the common practice of using a single **k** point in Car-Parrinello-type simulations. As an example, they find that if only one **k** point is used, a 108-atom cell would give a vacancy formation energy with the wrong sign, and even a 256-atom cell would give unacceptable results.

We have tested the effects of the system size on the unrelaxed vacancy formation energy using up to 216 atoms in

TABLE II. The unrelaxed vacancy-formation energies (in eV) as a function of cell size and band energy smearing. The **k** points for all runs are equivalent to a 182 **k**-point set.

Atoms per supercell	Structure	Equivalent **k** points	Band energy smearing (eV) 0.05 eV	0.20 eV	0.75 eV	1.6 eV	3.2 eV
1	fcc	182					
4	sc	56	0.737	0.736	0.743	0.749	0.748
8	fcc	28	0.752	0.755	0.770	0.778	0.752
16	bcc	20	0.753	0.750	0.761	0.746	0.739
27	fcc	10	0.655	0.689	0.763	0.780	0.751
32	sc	10	0.651	0.678	0.759	0.770	0.747
64	fcc	6	0.640	0.644	0.746	0.772	0.751
108	sc	4	0.691	0.661	0.748		
128	bcc	5	0.656	0.651	0.771		
216	fcc	2	0.640				

various supercell geometries and differing number of special **k** points in the irreducible Brillouin zone (IBZ). Table I shows the unrelaxed vacancy-formation energy of Al with cells containing up to 108 atoms for two sets of **k** points; the ''small'' and ''large'' sets being equivalent to 182 and 1300 **k** points, respectively, in the IBZ of fcc (primitive unit cell) Al. The Gaussian broadening factor[25] is fixed at 0.2 eV. We observe that there is remarkably little change in the vacancy-formation energy when the ''large'' set of **k** points is used. The unrelaxed vacancy-formation energy is relatively constant at 0.75 eV, varying by only 0.025 eV over the entire range from 4 atoms up to 108 atoms. However, if we use the smaller set of **k** points, the formation energy has observable changes as the system size increases. More importantly, there is a noticeable difference in the calculated energy for the 108-atom cell between the small (4) and large (20) sets of **k** points. Since the results of the large **k**-point set are settled to the order 0.01 eV from 32 to 108 atoms, there is good reason to believe that this is the converged result, which would imply that a 4-**k**-point sampling with Gaussian smearing of 0.2 eV is still inadequate for supercells as large as 108 atoms. These results indicate that a 108-atom cell, or even smaller, is already good enough for the point defect calculation, but the system with the vacancy is still a metal that requires adequate **k**-point sampling to give accurate results. A supercell of the order of 100 atoms is needed to allow a proper level of relaxation of the atoms near the defects due to the effects of the periodic boundary conditions.

We will now show that the stringent requirement for **k**-point sampling can be alleviated by using larger Gaussian broadening when the so-called ''entropy correction'' due to the smearing is taken into account as suggested by De Vita and Gillan.[26] All the calculated energies reported in this paper are computed with this correction. With this formulation, the error introduced by the Gaussian broadening is at most third order in the Gaussian smearing factor, so that for a fixed large set of **k** points the result of using large smearing is almost the same as using very small smearing. On the other hand, rapid convergence with respect to the number of **k** points is expected at large smearing, so that we may be able to obtain good results for metals with a smaller set of sampling **k** points if we use a large Gaussian broadening factor, as long as the entropy correction is taken into account properly. In Table II, we show the unrelaxed vacancy-formation energy using the small **k**-point set (equivalent to 182 **k** points in the IBZ of the primitive cell) using Gaussian broadening factors ranging from 0.05 to 3.2 eV. The results indicate that with large broadening, the results do approach those with the larger set of **k** points. For example, with a 108-atom supercell, a sampling of 4 **k** points and a smearing of 0.75 eV gives a calculated relaxed vacancy-formation energy of 0.748 eV, which compares favorably with the 0.735 eV obtained with 20 **k** points and 0.2-eV smearing. If we use 4 **k** points but a smearing of 0.2 eV, the result is 0.66 eV instead. These tests indicate that a larger Gaussian smearing can compensate for using fewer **k** points for the case of Al defect calculations.

However, care must be taken in choosing an appropriate level of smearing and an appropriate number of **k** points since there is a direct effect on the computational load and memory requirements. As the band energy smearing is increased, more bands need to be used in the calculation. More

TABLE III. The unrelaxed vacancy-formation energy (in eV) for Al_{16} as a function of band energy smearing and the number of **k** points.

Number of **k** points	Band energy smearing 0.05 eV	0.20 eV	0.75 eV	1.6 eV	3.2 eV
1	−4.346	−4.054	−3.123	−9.356	−6.162
4	−0.088	0.033	0.359	0.308	0.692
8	0.968	0.961	0.861	0.754	0.742
20	0.753	0.750	0.761	0.746	0.739
112	0.777	0.774	0.768	0.746	0.741

TABLE IV. Unrelaxed vacancy-formation energies comparing the pseudopotential method using 0.05- and 0.75-eV band energy smearing to an all-electron calculation by Mehl and Klein (Ref. 6) (all using a lattice constant of 4.05 Å).

Number of atoms	Number of **k** points	All-electron calculation (Ref. 6) (eV)	Pseudopotential (0.05-eV smearing) (eV)	Pseudopotential (0.75 eV smearing) (eV)
4	56	0.856	0.856	0.862
8	28	0.860	0.860	0.876
16	20	0.855	0.851	0.858
27	10	0.781	0.784	0.863
27	60	0.862	0.876	0.861

bands require more storage space and increase the computational load. Table II shows that the smaller set of **k** points reproduces the unrelaxed vacancy formation energy of 0.75 ± 0.02 eV range of the larger set when a moderate level of 0.75 eV smearing is used. This level of smearing increased the number of bands required by about 20%, which is a very small cost when compared to the cost of using more **k** points. Higher levels of smearing cannot reduce the **k**-point sampling much further, but do increase the cost of the calculation greatly. Increasing the smearing to 1.6 or 3.2 eV required many additional bands so that the increase in computational cost defeats the original purpose of using a high level of smearing.

Table III shows the vacancy-formation energy calculated for a cell with 16 Al sites as the number of **k** points are varied over a broader range. At a small Gaussian broadening of 0.05 eV, the results depend strongly on the number of **k** points used as expected, and a very large number of **k** points are needed to obtain reliable results. At the other extreme of using a large 3.2-eV broadening, the results converge with as few as 8 **k** points. When the set of **k** points is reasonably large, the results are rather independent of the Gaussian smearing factor. In fact, the results of the bottom row (112 **k** points at various Gaussian broadening) and the results of the last column (large broadening at various **k** points) are rather similar. This fact allows us to use a small **k**-point set with large broadening to obtain results similar to those of a large **k**-point set and small broadening (which is the correct result we are looking for). However, we should point out that if the **k**-point set is too small, in the limit of using just one **k** point as shown in Table III, the vacancy-formation energy is still hopelessly wrong no matter how much smearing is used. In this limit, there is simply insufficient information for a meaningful answer. In addition, we note that the high levels of 1.6- and 3.2-eV Gaussian broadening are almost as costly in the computation as using more **k** points, so little is gained. However, moderate levels of smearing, such as 0.75 eV, can provide high accuracy with fewer **k** points without adding much to the cost of the calculation.

The level of band energy smearing and the number of **k** points used affects the accuracy of the forces between the atoms in a manner similar to how the unrelaxed vacancy-formation energies are affected. The 4-**k**-point set with moderate smearing of 0.75 eV produces interatomic forces that are very close to the **k**-point converged forces. Lowering the number of **k** points or reducing the level of band energy smearing can cause deviations in the magnitude of the forces by up to 40%. However, it is interesting to note that even a sampling with only the Γ point and very small Gaussian smearing was able to find the equilibrium positions for the atoms to within 0.014 Å or 0.5% of the bond distance. Even though the forces may have been off by as much as a factor of 2, the atomic relaxation could still proceed to a rather accurate atomic configuration in this case. In short, we need a very careful sampling of **k** points to determine quantities such as vacancy-formation energy for metals, which by definition requires the comparison of the total energy of two different systems (one with the vacancy and one without). The **k**-point sampling must be adequate to give a reasonably good representation of the change of the local density of states about the defects before a reliable difference in energy can be established. The forces are gradients of the energy surfaces, and we found that they also require a good sampling. Equilibrium positions of the atoms in a system correspond to extremum of the energy surfaces. In the case of Al defects, we found that even though the forces are not accurate and the vacancy-formation energies are bad with single **k**-point sampling, the relaxed atomic positions are acceptable. This means that even though the energy surfaces have inaccurate absolute values and gradients, the extremum can be at more or less the same position as in the case with better sampling of the Brillouin zone.

With the effects of band energy smearing, system size, and choice of **k** points now understood, the optimal choice for accurately investigating the relaxed vacancy formation energy can now be made. A system of 108 Al atoms is large enough to allow for the relaxation of 4 shells of neighbors around the vacancy which should prove adequate. A choice of the 4 **k** points from the small set combined with the moderate level of 0.75 eV smearing of the band energy provides a high level of accuracy and proves to be computationally very efficient.

We note in passing that this technique of using larger broadening to compensate for fewer **k** points works well for simple metals, at least for the case of Al. However, care should be exercised before applying to transition metals, which have more structured density of states. We also note that earlier calculations of vacancy-formation energies showed some variations in the results[6,28,26] that have sometimes been attributed to the use of pseudopotentials in some of the calculations. In Table IV we show that our pseudopotential results can accurately reproduce the all-electron results of Mehl and Klein[6] if we use exactly the same lattice parameter (4.05 Å) and the same set of **k** points when a small

Gaussian broadening of 0.05 eV is used, and can reproduce the **k**-point converged results when a moderate smearing of 0.75 eV is used.

B. Vacancy-formation energy

The vacancy in aluminum has been used as a prototype system for point defects in simple metals, as well as a benchmark for computational methods. There have been many previous calculations of the vacancy-formation energy using methods ranging from pair potentials to local-density-functional methods, including both plane-wave pseudopotential and linear augmented plane-wave methods. LDA-based calculations employed periodic boundary conditions and earlier calculations have used relatively small supercells (16 to 32 atomic sites).[3,4,6,26] Since the relaxation surrounding a point defect in a supercell is constrained by the periodic boundary conditions, a sufficiently large unit cell should be used to model an isolated defect. Our use of 108 atomic sites in a simple cubic supercell puts the nearest distance between two single defects at about 12 Å and allows 4 shells of atoms to relax around the defect. Also, the availability of other theoretical and experimental results made this an ideal case for testing our approach to dealing with metallic systems.

The vacancy-formation energy is obtained from the difference between the total energy of the defect supercell with $N-1$ atoms and that of the perfect crystal with N atoms:

$$E_v = E(N-1,V') - \frac{N-1}{N}E(N,V). \tag{1}$$

We start from a perfect lattice consisting of 108 atoms on 108 lattice sites, remove one of the atoms to form the vacancy, and fully relax the positions of the ions. The lattice parameter of the cell is then varied followed by another complete relaxation of the ions. This is repeated to find the lattice constant and ionic configuration that produces a minimum in the total energy.

Using the 4-**k**-point set and 0.75-eV smearing of the band energy that was determined to be optimal for this problem, the fully relaxed vacancy-formation energy for 108 Al sites came out to be 0.66 eV. This is in good agreement with the experimental value of 0.67 ± 0.03 eV.[27] The vacancy-formation energy in Al has been studied carefully with large supercells by Chetty *et al.*,[8] who got basically the same result (0.66 eV) using a larger set of **k** points. Previous results with smaller supercells range from 0.52 to 0.84 eV.[6,28,26] Volume relaxation turns out to have only a small effect on the vacancy-formation energy as long as we allow for atomic relaxations around the vacancy site (this is not the case if relaxation is not allowed). If we fix the 108-atom cell at the equilibrium volume of Al, the vacancy-formation energy increases by only about 0.01 eV. This shows that atomic relaxation is much more important and the energetics of the defect formation is largely decided by the atomic configurations close to the vacancy. If no atomic relaxations were allowed, the vacancy-formation energy would be about 0.75 eV.

A vacancy-formation volume of $0.86\Omega_0$ was found using the definition of

$$\Omega^F = V' - (N-1)\Omega_0,$$

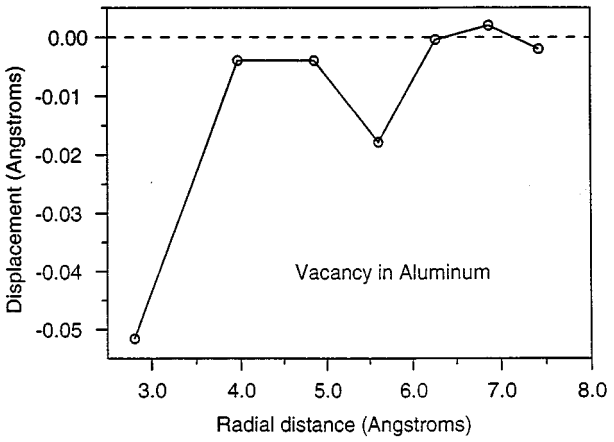

FIG. 1. The radial displacement for the atoms around a vacancy in aluminum. Shells 1 and 4, the face-center and face-diagonal, move inward while the other atoms remain roughly in place.

where Ω_0 is the volume of one atom in the perfect lattice and V' is the relaxed volume of the supercell with a vacancy. We note that Chetty *et al.*[8] obtained a value of $0.67\Omega_0$, while De Vita and Gillan,[26] using a smaller 16-atom cell, found $0.72\ \Omega_0$.

Figure 1 shows the lattice relaxation around the vacancy defect. Only the first four shells are completely free to move in response to the vacancy. The other shells are affected slightly by a small amount of contraction of the supercell but are at points equidistant between the defect and one of its periodic images and therefore cannot fully relax as they could around an isolated defect. It is mainly the first shell atoms that move inward by about 2% of the bond length to compensate for the vacancy. The fourth shell also shows significant displacement, more than the second and third shells. The first and the fourth shell atoms correspond to the face centered position and the positions diagonal across the face of the cubic cell. Therefore the lattice relaxation involves mainly a radial shift of the atoms along the face diagonals inward toward the vacancy site, as illustrated in Fig. 2. The other atoms remain in position aside from a slight

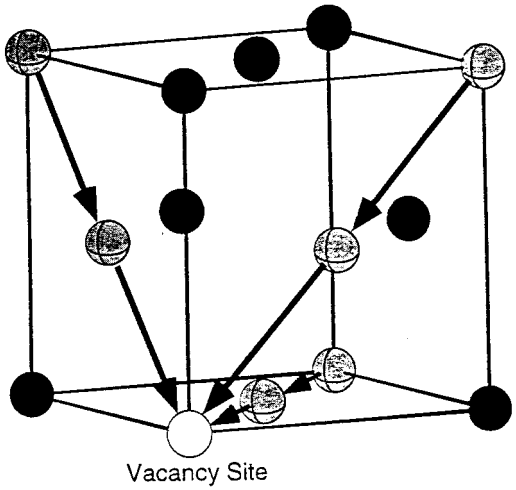

FIG. 2. Radial relaxation inward along the face diagonal for a vacancy defect in aluminum.

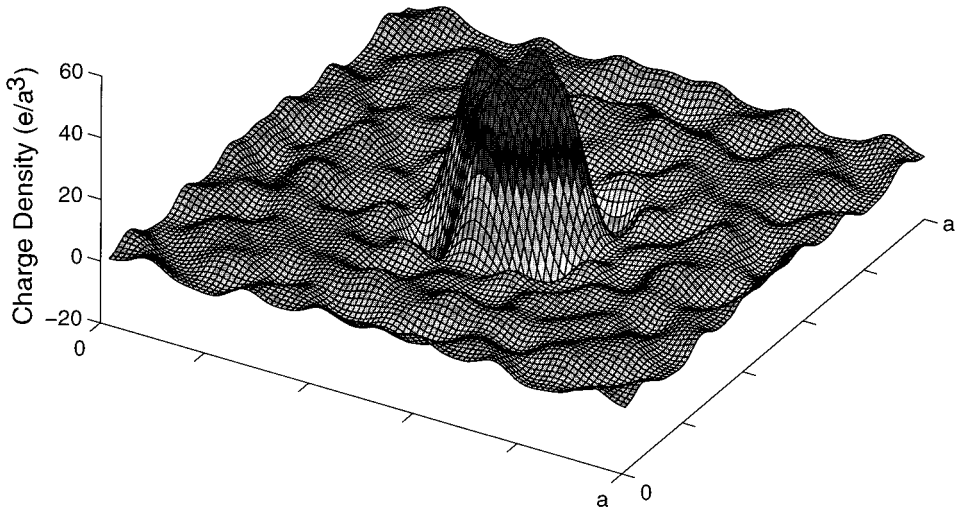

FIG. 3. The difference in electronic charge density in a vacancy defect in aluminum.

contraction of the supercell. A constant volume relaxation, where ionic and electronic relaxations are performed at a volume matching the bulk volume, produced very similar results since there is relatively little overall contraction of the system. The lattice relaxations we obtained closely match those of Chetty *et al.*[8] The Harris-functional local-orbital results of Caro, Drabold, and Sankey,[29] who also used up to 108-atom cells, found that the first shell of atoms moved inward by about 4% of the bond length (twice as big as ours), and the next two shells move outwards from the vacancy. However, these calculations did not allow for volume contraction and the lack of self-consistency in the Harris-functional approach may also contribute to the difference.

The plot in Fig. 3 shows the electronic charge density transfer that occurs when a vacancy is initially added to the bulk system. The figure shows the difference in charge density between the electronically relaxed system and the system of overlapping atomic charges for 107 aluminum atoms at the lattice sites. Clearly there is a flow of electrons into the vacancy site, which in turn provides the electrostatic force that pulls the neighboring ions in toward the vacancy.

C. Impurities in bulk aluminum

Li, Mg, and Si form important binary and ternary alloys with Al. It is therefore of practical interest to study the energetics of these elements embedded in an Al host. Since the conjugate-gradient method allows us to study systems with more than 100 atoms, the structural properties and the heats of formation of these elements in Al can be studied in the dilute limit. The heat of formation for a substitutional defect is defined here as the total energy of the two-component system minus the total energy of the same number of atoms of the constituent elements in the bulk environment:

$$H = E_{\text{host+impurity}} - E_i - \frac{N-1}{N} E_{\text{Al}(N)} . \qquad (2)$$

N is the number of sites in the unit cell, $E_{\text{host+impurity}}$ is the total energy of the unit cell containing $(N-1)$ host atoms and one impurity atom, E_i is the chemical potential of the impurity atom, which is taken to be the equilibrium bulk energy of the impurity, and $E_{\text{Al}(N)}$ is the energy of N Al atoms in the bulk environment. The bulk energy of the Al host is calculated with a 108-atom cell, with exactly the same **k**-point sampling and Gaussian broadening as the defect calculation to minimize systematic errors. We will consider Li, Mg, and Si as substitutional impurities, and a negative heat of formation indicates that the impurity is soluble in the low concentration limit, while a positive heat of formation indicates that the impurities will segregate. We employ a periodic cubic unit cell of 108 atoms, with 107 Al and one impurity atom. Both the volume and the atomic positions are fully relaxed. As in the case of vacancy calculations, we used 4 special **k** points in the irreducible Brillouin zone, and a Gaussian smearing of 0.75 eV. As a check, the heat of solution of Si in Al (without lattice and volume relaxation) with 20 **k** points and a Gaussian smearing of 0.2 eV is found to be 0.395 eV. With only 4 **k** points and 0.2-eV smearing, the result is 0.896 eV, which is obviously unacceptable. However, with the same 4 **k** points but a larger 0.75-eV Gaussian broadening, the heat of solution is found to be 0.400 eV, which is almost the same as that of the larger **k**-point set. In other words, what we have learned about **k**-point sampling in the vacancy-formation energy calculations is also applicable to the substitutional defect calculations.

The calculated heats and volumes of formation are listed in Table V. From these calculated heats of formation, we see that Li gains energy by substituting one Al atom in the Al host. On the other hand, the heats of formation of Mg and Si are positive. These results are consistent with available experimental information. The formation volume of the impurities is defined here as $V_F = V' - V_{\text{Al}(N)}$, where $V_{\text{Al}(N)}$ is the equilibrium volume of the Al host with N atoms, and V' is the total volume of a unit cell with $(N-1)$ Al atoms and one substitutional impurity. The formation volume is found to be positive for Mg and negative for Si and Li. According to published values of ''atomic and ionic radii,''[23] the sizes of the atoms decrease in the order Li>Mg>Al>Si. Thus, the trend we find is consistent with the atomic sizes for the case of Mg and Si. Since the heats of substitution are positive for these two elements, we may say that Mg and Si do not mix with Al in the dilute limit, and the volume expansion or

TABLE V. Single vacancy and substitutional defect formation energies for Li, Mg, and Si in bulk aluminum.

Defect	Formation energy (eV)	Formation volume	Chetty *et al.* (Ref. 8)	Experiment (Ref. 27)
Li	-0.496	$-0.107\Omega_0$		
Mg	0.038	$0.372\Omega_0$	0.07 eV	0.06−0.20 eV
Si	0.377	$-0.134\Omega_0$	0.37 eV	0.51 eV
Vacancy	0.664	$0.857\Omega_0$	0.66±0.03 eV	0.67±0.03 eV

contraction should largely be determined by atomic sizes. Li, on the other hand, dissolves in Al. The binding between the Li and the Al host draws the host metal atoms in and causes a contraction although bulk Li has a bigger atomic volume than Al. The lattice relaxations around the impurity are shown in Figs. 4(a)–4(c), for Li, Mg, and Si, respectively. For all three cases, the lattice relaxations are found mainly in the first shell of the Al atoms around the impurity site. The atoms in the first shell relax outward for Mg, and inward for Si and Li, which is consistent with the changes in the formation volume that Mg causes an expansion in the Al lattice, while Si and Li cause volume contractions. Our results for the lattice relaxation around a Si impurity agree well with those of Chetty *et al.*[8] The results of Caro *et al.*[29] agree qualitatively with ours, but their relaxations are substantially larger than the values we obtained.

D. Aluminum clusters

In the previous section, we have seen that it is energetically favorable for Li to substitute for Al in a bulk environment, but not so for Mg and Si. We will show that the situation can change quite a bit if we consider the same substitution in a small cluster environment.

All the calculations involving clusters were performed with an fcc supercell of lattice parameter $a=20$ Å, and a plane-wave cutoff of 12.5 Ry. By increasing the lattice parameter to 30.5 Å, we found that the total energy of an Al_{13} cluster changed by less than 1 meV, indicating that this supercell is large enough so that our results should be close to those of isolated clusters. Our calculations are not spin polarized (except for the atomic reference energy used below, where the spin polarization energies are calculated by an all-electron atomic Herman-Skillman type code), but the error of ignoring spin polarization should be small in clusters containing up to 13 atoms, especially when our attention is focused on clusters with ''magic'' numbers of electrons.

For the Al_{13} cluster, it is well known from theoretical calculations that the icosahedral cluster is lower in energy than the cubo-octahedral cluster,[30–34] although the reported energy differences varies from 0.6 eV (Ref. 31) to 1.6 eV (Ref. 32). Figure 5 shows both the icosahedral and cubo-octahedral clusters, with the center atom shaded darker. We find that ideal icosahedral Al_{13} ($I-Al_{13}$), with an optimized bond length of 2.76 Å and distance to center atom of 2.62 Å, is 1.02 eV lower in energy than cubo-octahedral Al_{13} ($O-Al_{13}$), which has an optimized bond length of 2.68 Å. Yi, Oh, ,and Bernhole[31] used a plane-wave pseudopotential Car-Parrinello scheme to find that ideal $I-Al_{13}$ is 0.6 eV

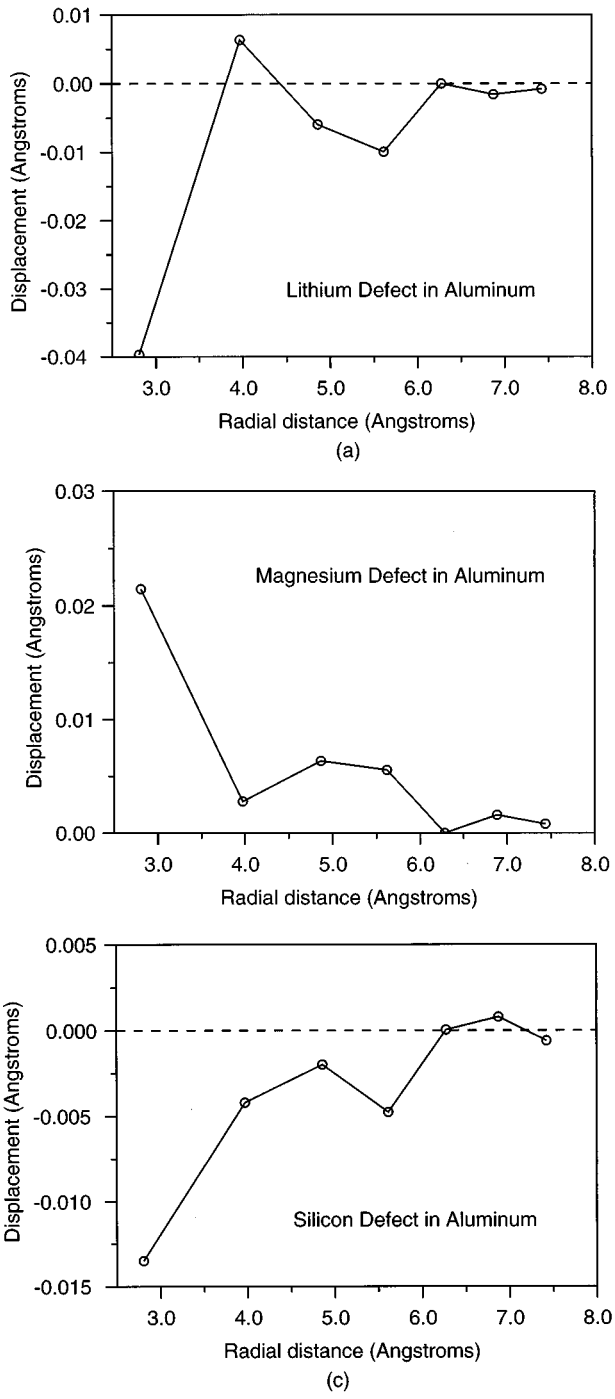

FIG. 4. The radial displacement for the atoms around a (a) Li, (b) Mg, and (c) Si substitutional defect in aluminum.

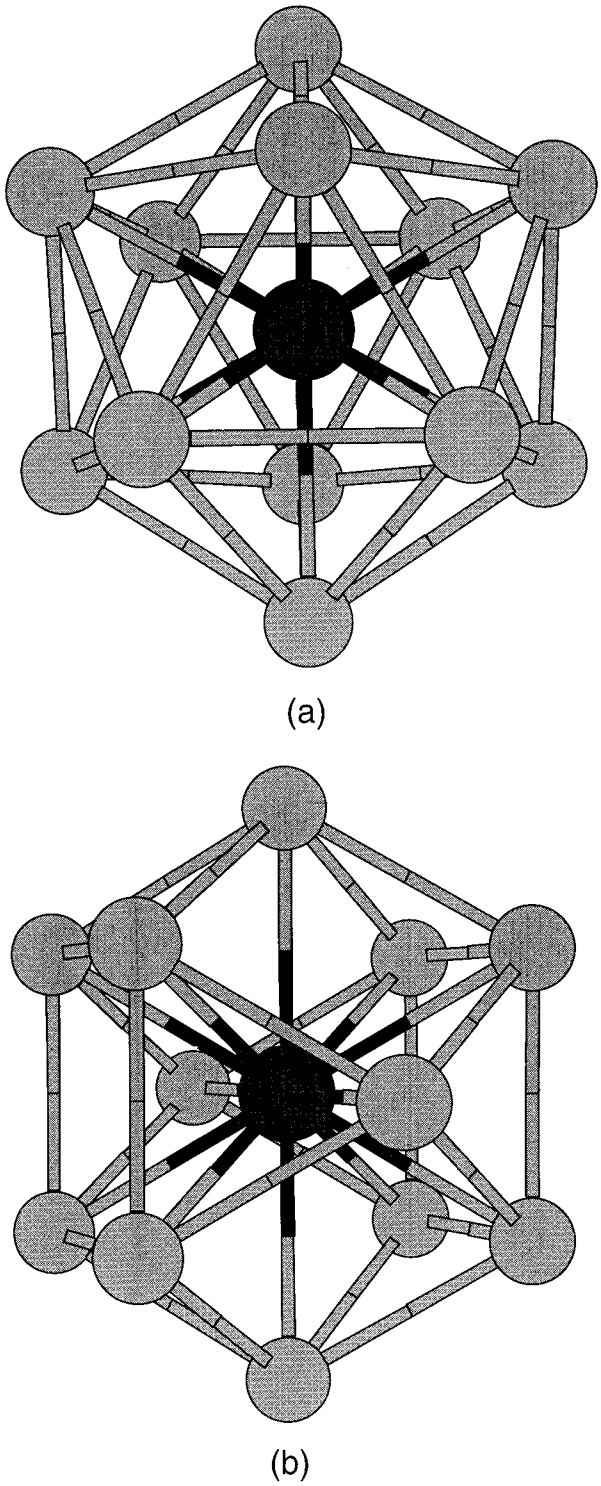

FIG. 5. (a) Icosahedral and (b) cubo-octahedral clusters with 13 atoms showing a different atom in the center.

lower than $O-Al_{13}$. This difference is due to the fact that Yi, Oh, and Bernhole used a much smaller 4-Ry plane-wave cutoff, which they estimated would lead to an error of 0.03 eV per atom, while we used a highly converged plane-wave cutoff of 12.5 Ry. Cheng, Berry, and Whetten[32] reported a much larger difference of 1.6 eV using an $X\alpha$ discrete variational method. Our result agrees well with that of Pederson,[34] who found an energy difference of 1.1 eV using an all-electron cluster code.

We now consider the change in binding energy when an Al atom is substituted by another atom, which is equivalent to the following substitution reaction:

$$Al_{13}+X\rightarrow Al_{12}X+Al. \tag{3}$$

X is Li, Mg, or Si, and is assumed to substitute the Al atom in the center of the icosahedral cluster. The icosahedral symmetry is maintained for both the Al_{13} and the $Al_{12}X$ clusters. Although these clusters may gain more energy by Jahn-Teller distortions, the energy gain is expected to be about 0.02 eV/atom,[31] which will not affect our results as discussed below. We found that the above interaction is highly endothermic for the case of Si, which gains an energy of 2.9 eV (Gong and Kumar[33] find a difference in binding energy of 3.2 eV). We also found that the interaction $2Al_{13}+Si_2\rightarrow 2Al_{12}Si+Al_2$ produces a gain of 2 eV, which further indicates the stability of the $Al_{12}Si$ cluster. On the other hand, the reaction is unfavorable for the case of Mg and Li, where the energy goes up by 3.5 and 2.6 eV, respectively. For an Al_{13} cluster, it is therefore energetically favorable for Si to substitute for an Al atom, but not so for the case of Li and Mg. The important point to note is that the trend is different from that of bulk behavior, where we found that it is favorable for Li to substitute Al, but not for Mg and Si. The distances of the Al atoms from the center impurity atom in the icosahedral clusters are 2.57, 2.59, and 2.64 Å for Li, Si, and Mg, respectively. In Al_{13}, the distance of the surface atom to the center atom is 2.62 Å. Mg thus causes an expansion of the Al cluster, while Si and Li cause contraction. This trend is consistent with the trend we found for substitution in the bulk.

The above results also hold for cubo-octahedral clusters. For example, $Al_{13}+Si\rightarrow Al_{12}Si+Al$ gains 2.2 eV when both Al_{13} and $Al_{12}Si$ are cubo-octahedral, while using Mg or Li instead of Si the energy goes up by 3.5 and 2.8 eV, respectively. $2Al_{13}+Si_2\rightarrow 2Al_{12}Si+Al_2$ produces a gain of 1.3 eV.

These results are therefore qualitatively the same as for the icosahedral and cubo-octahedral clusters, although these two forms have different structural characteristics. The observed trend in the energetics can be explained using a simple jellium model.[30,33] Al_{13} has 39 valence electrons, so it is one electron short of forming a closed shell of 40 electrons in the jellium sphere models.[35,36] This extra electron can be provided by substituting one Al by Si, but not by Mg or Li, accounting for the stability of $Al_{12}Si$. Since the stabilizing factor is electronic in origin, it is not surprising that we see the same trend for icosahedral and cubo-octahedral clusters, as long as they are both reasonably spherical. As the metal cluster size becomes bigger, and eventually grows into the bulk limit, the molecular energy levels are broadened into energy bands, and the highest occupied–lowest unoccupied molecular orbital gap will disappear. The contribution due to atomic relaxation to accommodate the defect becomes increasingly important and it will become more difficult to predict the trends of energetics. Whether an impurity atom will favorably substitute for the host in the bulk depends on

factors such as size mismatch and chemical bonding, which can in turn be attributed to the change in the electronic structure. It is quite difficult to predict these energetics based on simple arguments without doing a careful calculation. Even for the case of small clusters, the icosahedral cluster is uncharacteristically simple because of its high symmetry. In general, the problem can be very difficult even for a cluster of one component since the cluster may have a very complex potential energy landscape.

IV. SUMMARY

Using a preconditioned conjugate-gradient method, we have performed first-principles calculations to obtain the vacancy-formation energy of a single vacancy in aluminum and the energetics of Li, Mg, and Si substitutional impurities in bulk aluminum and small Al_{13} clusters. The calculated vacancy-formation energy and heats of solution are in good agreement with available experimental information. In the bulk point defect calculations, a supercell of about 100 atoms is found to be adequate for simulating isolated defects. However, **k**-point sampling needs to be done carefully and adequately for metallic systems. A higher level of band energy smearing was found to be beneficial by allowing the calculation to be performed with fewer **k** points without sacrificing accuracy. We found that the energetics of substituting an Al atom is rather different in the bulk and small cluster environments.

ACKNOWLEDGMENTS

We would like to thank Dr. B. C. Pan for checking some of our cluster results, and Dr. M. Weinert for helpful communications, especially about the issue of **k**-point sampling. This work was made possible in part by the Scalable Computing Laboratory, which is funded by Iowa State University and Ames Laboratory. Ames Laboratory is operated for the U.S. Department of Energy by Iowa State University under Contract No. W-7405-ENG-82. This work was also supported by the Director of Energy Research, Office of Basic Energy Sciences, U.S. Department of Energy. C.T.C. acknowledges support from DAG95/96-SC12 and HKUST694/96P from HKUST, Hong Kong. Z.Z.Z. acknowledges support from the China National Science Foundation and 863 Foundation.

*Electronic address: turner@ameslab.gov

[1] P.S. Ho, Phys. Rev. B **3**, 4035 (1971).
[2] G. Das, P.V.S. Rao, and P. Vashishta, J. Phys. F **5**, L35 (1975).
[3] R. Benedek, L.H. Yang, C. Woodward, and B.I. Min, Phys. Rev. B **45**, 2607 (1992).
[4] M.J. Gillan, J. Phys. Condens. Matter **1**, 689 (1989).
[5] R. Pawellek, M. Fahnle, C. Elsasser, K.M. Ho, and C.T. Chan, J. Phys. Condens. Matter **3**, 2451 (1991).
[6] M.J. Mehl and B.M. Klein, Physica B **172**, 211 (1991).
[7] P.T. Salo, K. Kokko, K. Mansikka, and R. Laihia, J. Phys. Condens. Matter **7**, 2461 (1995).
[8] N. Chetty, M. Weinert, T.S. Rahman, and J.W. Davenport, Phys. Rev. B **52**, 6313 (1995).
[9] P. Hohenberg and W. Kohn, Phys. Rev. **136**, B864 (1964); W. Kohn and L. J. Sham, *ibid*. **140**, A1133 (1965).
[10] R. Car and M. Parrinello, Phys. Rev. Lett. **55**, 2471 (1985).
[11] M. P. Teter, M. C. Payne, and D. C. Allen, Phys. Rev. B **40**, 12 255 (1989).
[12] I. Stich, R. Car, M. Parrinello, and S. Baroni, Phys. Rev. B **39**, 4997 (1989).
[13] M.C. Payne, M.P. Teter, D.C. Allen, T.A. Arias, and J.D. Joannopoulos, Rev. Mod. Phys. **64**, 1045 (1992).
[14] I. Stich, M.C. Payne, R.D. King-Smith, J.S. Lin, and L.J. Clark, Phys. Rev. Lett. **68**, 1351 (1992).
[15] K.D. Brommer, M. Needels, B.E. Larson, and J.D. Joannopoulos, Phys. Rev. Lett. **68**, 1355 (1992).
[16] J.S. Nelson, S.J. Plimpton, and M.P. Sears, Phys. Rev. B **47**, 1765 (1993).
[17] L. Hedin and B.I. Lundqvist, J. Phys. C **4**, 2064 (1971).
[18] Most of the calculations are done by minimizing the sum of eigenvalues for the lowest N states subject to the constraints that trial vectors are orthonormal. The set of vectors that optimize the sum of eigenvalues for a fixed number of N bands spans the same subspace as the N eigenvectors, but a subspace diagonalization is needed to rotate the subspace to that of the eigenvectors and find the eigenvalues of the individual levels. In our calculations of up to 108 atoms, the subspace diagonalization takes less than 5% of the computation time. However, when the system becomes larger, we can actually bypass the subspace diagonalization altogether. All we need to do is modify the minimization process. When the trial vector is updated, we normally orthogonalize the change vector to all the vectors in the current searching subspace. This just guarantees that the subspace is the same as that of the eigenvectors. However, if we explicitly orthogonalize the change vector to the eigenvectors of lower band index that are already known, then each vector optimized is in fact an eigenvector and subspace diagonalization is unnecessarily.
[19] D.H. Vanderbilt and S.G. Louie, J. Comput. Phys. **56**, 259 (1984).
[20] C.T. Chan, K.P. Bohnen, and K.M. Ho, Phys. Rev. B **47**, 4771 (1993).
[21] L. Kleinman and D.M. Bylander, Phys. Rev. Lett. **48**, 1425 (1982).
[22] R. Stumpf, X. Gonze, and M. Scheffler (unpublished).
[23] C. Kittel, *Introduction to Solid State Physics*, 6th ed. (Wiley, New York, 1986).
[24] D.E. Turner, Zizhong Zhu, C.T. Chan, and K.M. Ho (unpublished).
[25] C.L. Fu and K.M. Ho, Phys. Rev. B **28**, 5480 (1983).
[26] A. DeVita and M.J. Gillan, J. Phys. Condens. Matter **3**, 6225 (1991).
[27] P. Ehrhart, P. Jung, H. Schulta, and H. Ullmaier, in *Atomic Defects in Metals*, edited by H. Ullmaier, Landolt-Bornstein, New Series Group III, Vol. 25 (Springer-Verlag, Berlin, 1990).
[28] R.W. Jansen and B.M. Klein, J. Phys. Condens. Matter **1**, 8359 (1989).
[29] A. Caro, D. Drabold, and O.F. Sankey, Phys. Rev. B **49**, 6647 (1994).
[30] S.N. Khanna and P. Jena, Phys. Rev. Lett. **69**, 1664 (1992).
[31] J.Y. Yi, D. J. Oh, and J. Bernholc, Phys. Rev. Lett. **67**, 594 (1991).

[32] H.P. Cheng, R.S. Berry, and R.L. Whetten, Phys. Rev. B **43**, 10 647 (1991).
[33] X.G. Gong and V. Kumar, Phys. Rev. Lett. **70**, 2078 (1993).
[34] M. R. Pederson, in *Physics and Chemisitry of Finite Clusters: From Clusters to Crystals*, edited by P. Jena, S.N. Khanna, and B.K. Rao (Kluwer Academic, Dordrecht, 1992), Vol. II, p. 861.
[35] W.D. Knight *et al.*, Phys. Rev. Lett. **52**, 2141 (1984).
[36] M.Y. Chou and M.L. Cohen, Phys. Lett. **113A**, 420 (1986).